Industrial Crops & Products 223 (2025) 120296

Contents lists available at ScienceDirect

Industrial Crops & Products

journal homepage: www.elsevier.com/locate/indcrop

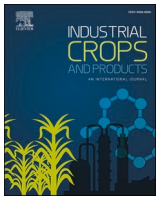

# Agricultural sustainability: Biochar and bio-based polyurethane coupling coating to prepare novel controlled-release fertilizers

Xin Tang [b,1], Jian Hua Li [a,1], Jia Yi Yang [c], Zhi Chao Xiang [b], Yan Ying He [b], Ying Zhen Huang [b], Nan Zhou [b], Wei Luo [c,d], Zhi Zhou [b,*]

[a] Hengyang Branch of Hunan Provincial Tobacco Company, Hengyang 421200, PR China
[b] School of Chemistry and Materials Science, Hunan Agricultural University, Changsha 410128, PR China
[c] College of Agronomy, Hunan Agricultural University, Changsha 410128, PR China
[d] National Center of Technology Innovation for Saline-Alkali Tolerant Rice, Changsha 410125, PR China

ARTICLE INFO

*Keywords:*
Waste utilization
Biochar
Bio-based polyurethane
Controlled-release fertilizer
Agricultural sustainability

ABSTRACT

The application of bio-based controlled-release fertilizers is one of the sustainable methods for improving fertilizer effectiveness and reducing agricultural non-point source pollution. In this study, liquefied tobacco (*Nicotiana tabacum* L.) stem (LTS) and castor oil were used as raw materials to prepare bio-based polyurethane coating (BPC). The BPC and biochar obtained through pyrolysis were coated on nitramine phosphorus to prepare bio-based double-coated controlled-release fertilizers (BDCRFs). The variables are the 3 %, 5 %, and 7 % BPC coating amounts and biochar from different sources (tobacco stem, fir wood and coconut shell were pyrolyzed at 500 ℃ under oxygen restriction) as components of BDCRFs. The results demonstrated that the excellent hydrophobicity (water contact angle = 138°) and lipophilicity (polyols contact angle = 30°) of tobacco stem biochar (TSB) was conducive to coupling with BPC to improve the controlled-release performance of BDCRFs. Column leaching test indicated the tobacco stem fertilizer (TSF) can achieve long-term controlled-release: with the coating rate of 3 %, 5 % and 7 %, TSF released 71 % ± 2 %, 66 % ± 2 % and 71 % ± 2 % of nutrients on 70, 84 and 124 days, respectively. Meanwhile, the kinetic analysis revealed that the nutrient release mechanism of BDCRFs followed the Ritger-Peppas model. Additionally, TSF with the excellent nutrient release performance were compared with conventional fertilizer (CF), nitramine phosphorus (NP), and no fertilizer (CK) in tobacco field experiments. The results indicated that the biomass, growth indexes and nutritional status of tobacco reached the highest under TSF-5 % treatment. Therefore, the nutrient release of BDCRFs matched the nutrient demand for tobacco growth, reducing the time and labor costs of topdressing and improving the nutrient utilization rate. Therefore, BDCRFs are considered as potential candidates for sustainable development of agriculture and the widespread development and application of controlled-release fertilizers.

## 1. Introduction

The agricultural sector is currently confronted with the significant challenge of striking a balance between enhancing productivity and ensuring environmental sustainability. The extensive application of fertilizers plays a crucial role in enhancing soil fertility and boosting crop yields (Zhang et al., 2018). However, conventional fast-effective fertilizers have problems such as poor nutrient utilization efficiency and uncontrollable slow-release behavior. Leaching of nutrients (mainly N, P and K) contributing to a range of environmental issues such as water eutrophication, soil compaction and salinization (Hu et al., 2024). The average utilization rates of N, P and K in Chinese crops were only 33 %, 24 % and 42 %, respectively. In recent years, controlled-release fertilizers (CRFs) have attracted significant attention to improve nutrient utilization and reduce environmental pressure. Fertilizer polymer coating technology has demonstrated the potential to deliver nutrients at a slow/controlled-release rate more effectively, achieving optimal crop nutrition while minimizing environmental issues (Kassem et al., 2024). Most coating materials used in CRFs are predominantly petroleum-based products such as polyvinyl alcohol, polyurethane and

* Corresponding author.
*E-mail address:* zhouzhi@hunau.edu.cn (Z. Zhou).
[1] co-first author

https://doi.org/10.1016/j.indcrop.2024.120296
Received 25 October 2024; Received in revised form 5 December 2024; Accepted 8 December 2024
Available online 12 December 2024

polyolefin etc. These materials are costly and pose challenges in terms of degradation, which significantly restricts the widespread application of CRFs (Zhang et al., 2021). In addition, the EU's regulatory activities on plastics may also affect the use of traditional coatings on fertilizers (Nielsen et al., 2023). It has been reported that polyols can be derived from biomass liquefaction technology, and then cheap, renewable and degradable bio-based polyurethane coating materials can be synthesized with isocyanate (Wang et al., 2021). Ma et al. used cotton straw and siloxane to prepare superhydrophobic bio-based polymer coated fertilizer, The nitrogen release time of 7 % of the coated fertilizer reached 38 days (80 % release) (Ma et al., 2018). Diego et al. coated phosphate fertilizer with castor-based polyurethane, and the maximum release time of the fertilizer reached 44 days (80 % release) (da Cruz et al., 2017). Chen et al. prepared bio-based polymer-coated fertilizer by liquefaction of lignin. The coated fertilizer results in 70 % phosphorus release after 21 days (Chen et al., 2023). The bio-based CRFs reported above all exhibited effective controlled-release of fertilizers.

Tobacco, as a high-value crop, is widely cultivated in China with an annual production of about 5 million tons (Ma et al., 2022). As a part of tobacco, tobacco stem (TS) is usually regarded as tobacco field waste to be discarded or incinerated, causing resource waste and environmental pollution (more than 48 million kilograms of tobacco stems were produced in 2017) (Muvhiiwa et al., 2021). However, owing to high content of cellulose, hemicellulose and lignin in TS, it has the potential to prepare liquefied polyols for the synthesis of bio-based polyurethane coatings (BPC) (Brzoska et al., 2024). The majority of CRFs produced by BPC exhibits inadequate nutrient release characteristics as a result of the abundance of hydrophilic groups and pores (Ma et al., 2018; Wang et al., 2023). In order to address the limitations of BPC, hydrophobic and thermostable additions such as organic siloxane (Zhang et al., 2021) and nanoparticles (Zhang et al., 2017) were grafted with hydrophilic groups in BPC to enhance the controlled-release performance of CRFs. Nevertheless, the high cost of these additives and the environmental pollution associated with the application in soil have limited the large-scale implementation of additives. Biochar is widely considered as a cost-effective and environmental-friendly material. On the one hand, biochar is applied directly in soil to enhance soil properties, including pore structure, cation exchange capacity, pH, and salinity regulation (Zhang et al., 2022). On the other hand, it can also serve as a coating layer or additive to enhance the degradability and mechanical strength of polymer coatings, consequently facilitating the long-term stable controlled-release of CRFs (González et al., 2015; Jia et al., 2020). Therefore, CRFs prepared with biochar have significant potential for enhancing the controlled-release properties of fertilizers and soil improvement applications.

Herein, a hypothesis has been proposed: the coupling of biochar and bio-based polyurethane both derived from biomass can enable long-term controlled nutrient release and enhance fertilizer efficiency. To certify the hypothesis, the bio-based double-coated controlled-release fertilizers (BDCRFs) were successfully prepared with bio-based polyurethane and biochar as raw material. Biochar materials derived from low-cost bio-wastes (fir wood (FW), tobacco stem (TS), coconut shell (CS)) are characterized to explore its applicability in the development and utilization of CRFs. The results demonstrated that tobacco stem biochar has hydrophobicity (water contact angle of 138°) and lipophilicity (polyol contact angle of 30°), which is conducive to BPC coupling. Liquefied tobacco stem (LTS), produced through the liquefaction of tobacco stems, are utilized to synthesize a bio-based polyurethane coating (BPC), which is then characterized for its degradability (16 % degradation in 120 days). The synthesis of BDCRFs involved coating biochar on nitramine phosphorus particles, followed by the polymerization of LTS and isocyanate on the biochar surface. The BDCRFs were comprehensively characterized, and the nutrient controlled-release performance of BDCRFs was evaluated, with the nutrient release mechanism revealed through kinetic analysis (Ritger-Peppas model). The controlled release of TSF-3 %, TSF-5 % and TSF-7 % released 71 % ± 2 %, 66 % ± 2 % and 71 % ± 2 % of nutrients on 70, 84 and 124 days, respectively. Finally, field experiments were conducted to prove the application of TSF could meet the nutrient demands of tobacco growth, reduce topdressing time and labor costs, and significantly enhance nutrient utilization rates, thereby realizing the cyclic utilization of tobacco field wastes. The environmentally friendly, low-cost, and high-performance BDCRFs holds promise for addressing challenges such as low fertilizer use efficiency, high application costs, leaching losses, and potential environmental contamination from coating materials. Furthermore, it provides technical and theoretical foundations for the sustainable development of agriculture and the widespread development and application of CRFs.

## 2. Materials and methods

### 2.1. Materials

Tobacco stem (TS), collected from the Changsha Liu Yang tobacco trial site, was dried at 105 ℃ for 24 h to remove moisture content, then crushed and screened through a 60-mesh sieve. Fir wood (FW), collected from a wood factory in Guizhou. Coconut shell (CS), collected from a biomass pellet factory in Hainan. Castor oil, polyethylene glycol (PEG-400), glycerol, Polyvinyl Alcohol (PVA) and attapulgite powder were obtained from Shanghai Macklin Biochemical Technology Co., Ltd. Polyaryl polymethylene isocyanate (PAPI) was purchase from Sinopharm Chemical Reagent Co., Ltd. Nitramine phosphorus (already screened, 3 mm in diameter and nitrogen content 30 %) was obtained from Hunan Jin Ye Zhong Wang Technology Co., LTD.

### 2.2. Preparation of biochar

The preparation process of biochar as shown in Fig. 1a. A 300 mL ceramic crucible was filled with 50 g of TS, covered, and then placed into a Muffle furnace. The crucible was heated from room temperature to 500℃ for 2 h. After the temperature dropped to room temperature, the crucible was removed and the prepared tobacco stem biochar (TSB) was collected. The fir wood biochar (FWB) and coconut shell biochar (CSB) were prepared under the same conditions as above.

### 2.3. Preparation of liquefied tobacco stem

The scheme of liquefaction progresses for TS as shown in Fig. 1b. The liquefaction of TS was implemented in a 1000 mL three-neck flask with condenser, electric stirrer and thermometer fitted. PEG-400 (280 g) and glycerol (120 g) were Poured into the flask with stirring constantly. The flask was then heated to 160℃ and 80 g of TS was added into the flask mixed with the liquefaction agents. Finally, the sulfuric acid (12 mL) was gradually dripped into the flask. Most of TS was liquefied after 90 min, and then the solid-liquid mixture was removed and filtered to obtain polyol solution after the flask was cooled at room temperature. The liquefied tobacco stem (LTS) was saved for the subsequent preparation of fertilizer coating materials. The solid obtained from the filtration was dried and weighed to calculate the liquefaction rate.

### 2.4. Preparation of bio-based fertilizer coating material

Mixed polyols were prepared by mixing CO and LTS according to mass ratio 4:1 for 10 min. 1 g mixed polyol was mixed with 1 g PAPI and stirred for 1 min for polymerization reaction, and then added polymerization solution into the polytetrafluoroethylene mold evenly, and then cured in the oven at 75℃ for 30 min to form a film. The bio-based polyurethane coating (BPC) was obtained (The thickness of BPC is about 200 μm, which is consistent with the thickness of the characterized fertilizers).

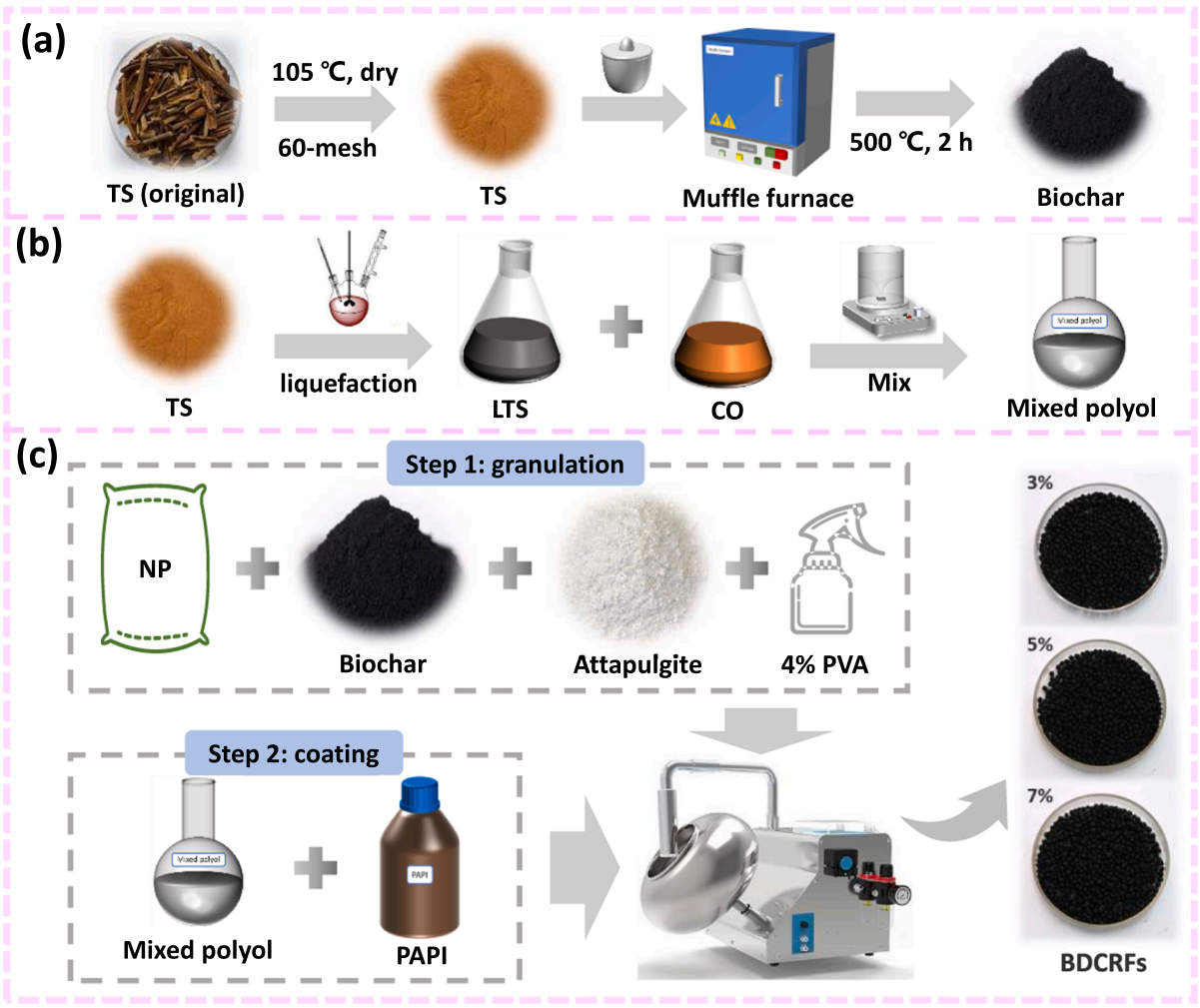


**Fig. 1.** The scheme of preparation progresses for (a) biochar, (b) mixed polyol, (c) BDCRFs.

### 2.5. Preparation of BDCRFs

The scheme of preparation progresses for BDCRFs as shown in Fig. 1c. The BDCRFs were named as FWF-X, TSF-X and CSF-X (X is the coating content of polyurethane: 3 wt%, 5 wt% and 7 wt%) according to the type of biochar and amount of coating. 300 g of nitramine phosphorus (3 mm in diameter and nitrogen content 30 %) was placed in a rotary coating machine (BY-300, Shanghai Drug testing Instrument Co., LTD) and the rotation speed of the coating machine was 30 r/min. Then 20 wt% (The mass ratio was calculated according to the total amount of fertilizer, the same below) biochar and 5 wt% attapulgite were added to the coating machine to mix evenly (10 min). Then 3 wt% PVA aqueous solution (4 %) was sprayed into the coating machine as a binder for granulation. After granulation, mixed material was preheated at 75℃ for 10 min. The mixed polyol (1.5 wt%) and PAPI (1.5 wt%) described in 2.4 were added to the coating machine three times (0.5 wt% BPC and 0.5 wt% PAPI were added each time), each reaction was 10 min, and after three reactions (30 min), the coating amount of 3 wt% BPC was formed. The preparation steps for coating amounts of 5 % and 7 % were the same as above, but the addition of mixed polyols was added at 5 wt% and 7 wt% respectively. In addition, we obtained an economic evaluation of BDCRFs by calculating the market price of the above-mentioned materials and the energy (mainly electricity) used in the preparation process (Zhu et al., 2024). The production prices of BDCRFs in different coating amounts were compared with representative commercial CRFs (Table 3).

### 2.6. Characterization analysis

The fundamental properties (pH, EC, BET, et al.) of biochar were measured according to NY/T 3672–2020. A thermos gravimetric analyzer (TGA, Mettler Toledo, Switzerland) was used to analyze the thermal stability of biochar. 10 mg of sample was heated from 50 ℃ to 700 ℃ at 10 ℃/min in air (flow rate = 100 mL/min). The graphitization degree of biochar was conducted by employing the Raman spectrometer using a 532 nm laser wavelength. The water contact angle (WCA) of biochar surfaces were determined by the droplet shape analyzer (KINO SL200KS, American). Fourier-transform infrared (FTIR, Nicolet 380, American) spectroscopy was used to analyze the surface functionality of biochar, TS, LTS and BPC. The scanning electron microscope (SEM, Quanta250FEG, USA) was used to determine the surface morphology of biochar and CRFs. The acceleration voltage was set to 5 kV, the scanning mode was secondary electronic mode, and the vacuum is $10^{-3}$ pa. The sample was fixed on the sample table with conductive tape, and the fertilizer cross section detection was obtained by cutting the fertilizer particle from the center with a scalpel to expose the cross-section morphology. The atomic force microscope (AFM, Bruker multimode, German) was used to analyze the surface roughness of controlled-release fertilizer. The contact mode is semi-contact mode, and the scanning range is 5 × 5 microns. The composition and molecular weight distribution of LTS were determined using a gas chromatography-mass spectrometer (GC-MS, Agilent, 6890 N/5975B, America) and a gel permeation chromatograph (GPC, model HLC-8420, Japan), respectively. Specific parameter settings for GC-MS and GPC determination of

LTS were further described in supplementary materials (Text S1). The biodegradability of BPC was measured. The soil burial degradation was conducted according to the method of Chen et al. (2018) (Chen et al., 2018). The dry BPC pieces (3 × 3 cm, thickness 0.1–0.3 mm) were buried in soil at a depth of 10 cm. Sprinkle about 15 mL of water every 3 days to keep the soil moist. The soil biodegradation test was carried out for 120 days at regular intervals (10 days). Remove the samples carefully from the soil and rinse with distilled water to remove the soil. The samples were then dried at 60 °C at a constant weight. At each sampling, three samples were washed and weighed to calculate the mass loss. The surface morphology of the BPC after 120 days of degradation was analyzed by scanning electron microscope (SEM, Quanta250FEG, USA). Nitrogen responsiveness (biochar exhibits adsorption or release of nitrogen) of biochar was measured. 0.1 g of biochar was added into 250 mL conical bottle and 100 mL of ultra-pure water (or add 50 mg/L of ammonium chloride solution) was added, then the conical bottle was put into a shaker (150 rpm, 25℃) for 24 h and removed. The biochar was filtered and the filtrate was collected for determination of nitrogen content. The automatic mobile injection analyzer (FIA-6000 +, China) was used to determine the total Kjeldahl nitrogen content in fertilizer solution and tobacco plants. The detection wavelength was 660 nm, the temperature of the heating module was constant at 37 ℃, the rotational speed of the peristaltic pump was 35 r/min, the integration method was calculated according to the peak area, and the injection time was 50 s. The treatment of tobacco samples, fertilizer samples and the preparation of the solution required for testing are described in Text S2.

### 2.7. Column leaching of BDCRFs

The cumulative N release rate of FWF, TSF and CSF in quartz sand columns at 25℃ was determined (refer to GB/T 41667-2022). The leaching test device was a PVC cylindrical tube (35 cm height, 5 cm inner diameter). Each column with 30 cm of quartz sand (no other impurities) and two fine nylon screens were placed at the bottom of the column to prevent quartz sand from entering the leachate. The 10 g fertilizers were put into a net bag, and then placed the bag in the middle of the quartz sand. Each treatment was repeated three times. The deionized water (100 mL) was added to the top of the column for each test. The leachate at the bottom of the column was collected for subsequent determination. Leaching was performed on 1, 3, 5, 7, 10, 14, 28, 42 and 56 days. The water samples were collected and nitrogen concentration was determined (Nitrogen determination methods are described in 2.6), until the N release rate reached 80 %.

### 2.8. Nutrient release kinetics

Three dynamic equations were used to fit the nutrient release of controlled-release fertilizers: the zero-order kinetic equation, the first-order kinetic equation, Higuchi kinetic equation and Ritger-Peppas kinetic equation (Mohamed et al., 2022; Papadopoulou et al., 2006).

Zero-order kinetic equation:

$$N_t = a * t + b \tag{1}$$

First-order kinetic equation:

$$\frac{N_t}{N_0} = 1 - \exp\hat{}(-kt) \tag{2}$$

Higuchi kinetic equation:

$$\frac{N_t}{N_\infty} = K_H * \sqrt{t} \tag{3}$$

Ritger-Peppas kinetic equation:

$$\frac{N_t}{N_\infty} = Kt^n \tag{4}$$

where $N_t$ is the cumulative release rate in time $t$, $N_0$ is the maximum release rate, $N_t/N_\infty$ is the release rate at time $t$. $a$, $k$, $K$ and $K_H$ is the diffusion kinetic constant in each equation, $b$ is the release constant, $n$ is the diffusional exponent.

### 2.9. Field experiment

Field experiment was performed to study the effects of BDCRFs on crop growth. The field experiment was conducted in tobacco experimental field in Liu Yang, Changsha, Hunan Province. The planting soil was loamy sandy soil with pH 6.14, organic matter 14.27 g/kg, available phosphorus 54.49 mg/kg, alkali-hydrolyzed nitrogen 181.34 mg/kg, and cationic exchange capacity 17.58 cmol/kg. Fertilizers were applied 14 days before tobacco transplanting. CK was treated with no fertilizer; CF was treated according to local conventional fertilization (The sample in this work is the local second topdressing data, and the local total of four topdressing times); NP was treated with uncoated nitramine phosphorus. Each treated with two ridges, a total of 12 ridges, and the total planting area was 0.075 $hm^2$. The ratio of nitrogen, phosphorus and potassium per hectare was 150: 180: 480 in local fertilization. For CF, base fertilizer (1050 kg/$hm^2$) and cake fertilizer (600 kg/$hm^2$) were used as fertilizer before tobacco transplantation, and potassium sulfate (450 kg/$hm^2$) and potassium nitrate (450 kg/$hm^2$) were applied in the following four topdressing times. The ratio of nitrogen, phosphorus and potassium applied in NP and CRFs groups was the same as CF. Nitrogen fertilizer was provided by nitramine phosphorus (502.5 kg/$hm^2$), phosphate and potassium were provided by calcium magnesium phosphate fertilizer (1500 kg/$hm^2$) and potassium sulfate (922.5 kg/$hm^2$), respectively. Tobacco was transplanted on 15 March, 2024, with rows spaced 120 cm apart and plants spaced 50 cm apart. Agronomic traits of tobacco were measured and sampled during the budding stage. The roots, stems and leaves of the plants were collected and washed with distilled water, then dried with absorbent paper, and the fresh weight of the roots, stems and leaves was measured. The samples were then dried in an oven at 105 °C for 30 min, followed by drying at 60 °C to a constant weight, after which the dry weight was measured. Finally, the nitrogen content of the plants was measured and calculated. Each treatment was repeated three times.

### 2.10. Statistical analysis

Data were recorded and organized using Microsoft Excel 2021 (Microsoft, Washington, USA). Statistical analysis was performed using IBM SPSS 26 (SPSS, Chicago, USA), one-way analysis of variance (ANOVA) followed by the least significant difference (LSD) method was used to compare the significance of differences between treatments, with significance levels of $p < 0.01$. Data were visualized and plotted using Origin 2022 (Origin Lab, Massachusetts, USA). The synthesis reaction diagram of tobacco stem liquefaction and polyurethane was drawn with king draw (Qingdao Qingyuan Precision Agriculture Technology Co., LTD, Qingdao, China).

## 3. Results and discussion

### 3.1. Characterization of biochar

Table 1 showed the agronomical and surface properties of the FWB, TSB and CSB. All the biochar exhibited alkalinity (The pH of FWB, WSB and CSB reached 8.35 ± 0.21, 9.01 ± 0.29 and 7.89 ± 0.09, respectively) due to the hydrolysis of alkali salts and alkaline elements such as calcium (Ca), magnesium (Mg), sodium (Na) and potassium (K) (Pariyar et al., 2020). The alkaline biochar has potential applications in acidic soil improvement (Prasad et al., 2018). Compared with FWB and TSB, CSB has a higher electric conductivity (EC) due to its higher soluble salt content and higher specific surface area (Dugdug et al., 2018). The CEC indicates the ability of biochar or fertilizer to absorb nutrients (cations).

**Table 1**
Agronomical and surface properties of biochar.

| Sample | pH | EC (μs/cm) | CEC (cmol/L) | TOC (mg/g) | BET ($m^2$/g) |
|---|---|---|---|---|---|
| FWB | 8.35 ± 0.21b | 31.90 ± 1.15c | 12.69 ± 0.58b | 475.12 ± 1.53c | 164.81 ± 1.15b |
| TSB | 9.01 ± 0.29a | 47.80 ± 0.80b | 28.24 ± 1.38a | 495.57 ± 0.77a | 139.60 ± 2.62c |
| CSB | 7.89 ± 0.09b | 117.20 ± 1.21a | 13.88 ± 0.47b | 484.23 ± 0.56b | 1454.17 ± 2.71a |

TSB has the highest CEC (28.24 ± 1.38 cmol/L) compared with FWB and CSB. The high CEC of biochar contributes to fix nutrient elements ($K^+$, $NH_4^+$) in soil and promotes the absorption of nutrients for plants (Bera et al., 2017). In addition, the FWB, TSB and CSB have higher total organic carbon, and the application of biochar into soil is conducive to increasing soil organic carbon content. The content of heavy metal elements in biochar was determined, as shown in Table S2. The total concentrations of all heavy metal elements (As, Cr, Co, Cu, Pb, Ni and Zn) detected in the FWB, TSB, and CSB were far below the allowable thresholds specified by the International Biochar Initiative (Sun et al., 2023). Therefore, the application of FWB, TSB and CSB into soil will not cause secondary pollution. The surface morphology of biochar was analyzed by SEM as shown in Fig. S1. The results showed that all biochar had sheet (block) structure. FWB and TSB have circular hole defects, while CSB has strip defects, which was can be attributed to the volatilization of organic matter during the pyrolysis process (Shaaban et al., 2013). These defects are conducive to increasing the specific surface area of biochar, which improving soil structure and properties such as porosity and water retention after application (Marcińczyk and Oleszczuk, 2022).

The results of TGA and DTG indicated that the thermal stability of the biochar followed the order: CSB > FWB > TSB (Fig. 2a). This was due to the higher carbonization degree of CSB and FWB. This difference was reflected by the higher BET surface area of CSB (1454.17 ± 2.71 $m^2$/g) and the higher carbon content of FWB (77 %) (Carneiro et al., 2018). Raman spectroscopy was used to analyze the crystallinity and graphitization degree of biochar, as shown in Fig. 2b. The ID/IG value was commonly used to measure the degree of defects in biochar (Dong et al., 2022). The result had shown that TSB has the least degree of defects and higher degree of graphitization (ID/IG = 1.534), which also related to the different carbonization degrees of biochar prepared by pyrolysis with different raw materials. The results of FTIR analysis (Fig. 2c) showed that FWB, TSB and CSB all contain -OH (3433 $cm^{-1}$), -C═O (1610 $cm^{-1}$), -COOR (1190 $cm^{-1}$), -R-O-R' (1035 $cm^{-1}$). The $-CH_3$ or $-CH_2$- (1435 $cm^{-1}$) was present in FWB and TSB, while $-CH_3$ is a hydrophobic group, so FWB and TSB will exhibit stronger hydrophobic properties than CSB. The response of biochar to nitrogen was measured (Fig. S2). It can be seen that there was a certain degree of nitrogen release in FWB and CSB, while TSB has an adsorption effect on nitrogen. On the one hand, FWB and CSB can provide more nutrients for crops, and on the other hand, TSB can be used as biochar-based fertilizer to further improve the control of fertilizer release.

The water absorption and water contact angle (WCA) of FWB, TSB and CSB were shown in Fig. 2d. Hydrophobicity was defined as the water contact angle more than 90° and vice versa. The preparation temperature and type of biochar will affect the type and quantity of surface functional groups, and then affect its hydrophobicity (Fan et al., 2022; Sun et al., 2022). The WCA value of FWB, TSB, and CSB all greater than 90°, indicating all the biochar exhibited hydrophobicity. The WCA of FWB and TSB reached 137° and 138° respectively, showing higher hydrophobicity compared with CSB. This can be attributed to the CSB

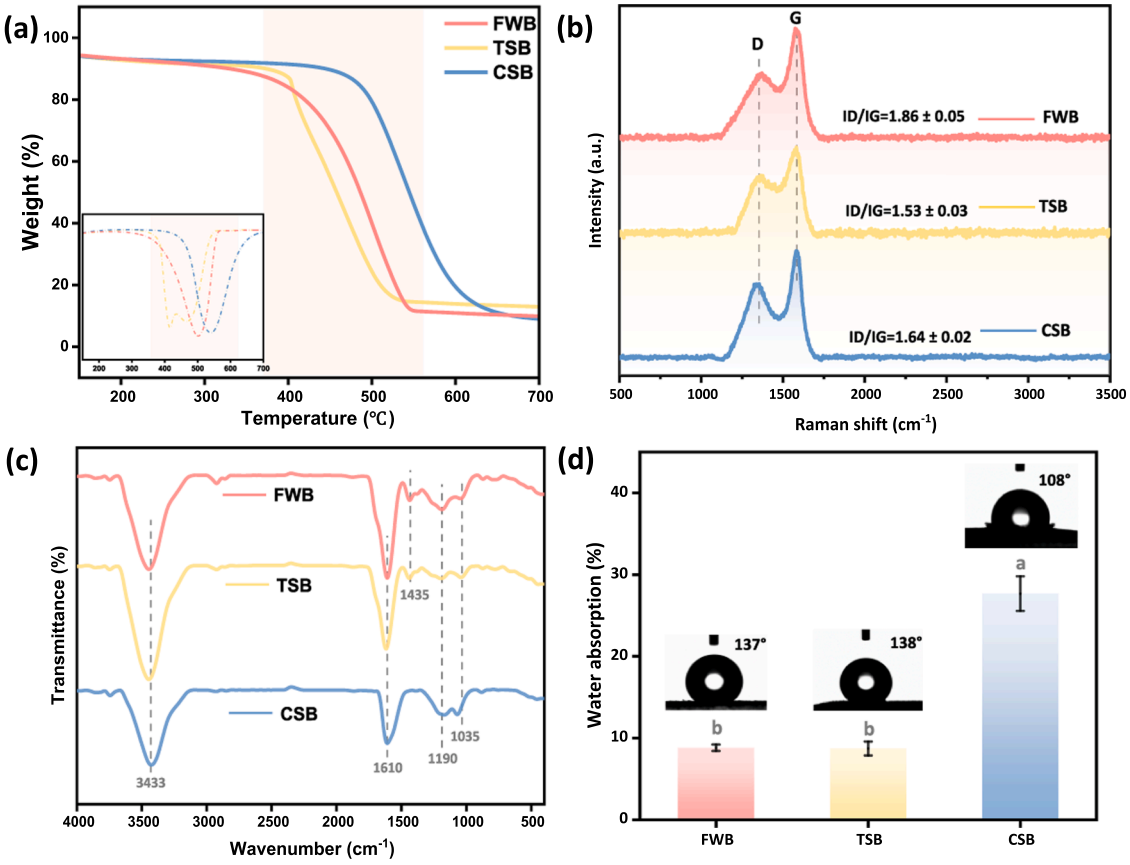


**Fig. 2.** (a) Thermogravimetric analysis of biochar. Note: The inset represents the derivative plot. (b) Raman analysis of biochar. (c) FTIR analysis of biochar. (d) The water absorption capacity and water contact angle of biochar.

has a higher specific surface area and larger pore structure leading to easier infiltration of water (Dong et al., 2023). In addition, the WCA and water absorption of biochar showed obvious correlation, while the higher the WCA, the lower the water absorption. The results showed that all three kinds of biochar showed hydrophobicity, especially the hydrophobic angle of TSB reached 138°, indicating that the addition of biochar in controlled-release fertilizer was conducive to enhancing the hydrophobicity of fertilizer and improving the controlled-release performance of fertilizer. The lipophilic property of biochar was measured using diiodomethane, PVA aqueous solution (4 %) and mixed polyol (CO: LTS = 4:1 wt%), respectively (Fig. S3). Compared with FWB and CSB, TSB exhibited the largest lipophilicity in diiodomethane and mixed polyol, indicating TSB was more easily combined with coating materials (BPC) to improve the coating layer density in the process of fertilizer preparation, so as to further enhance the controlled-release performance of fertilizer (Jia et al., 2020; Madhubashani et al., 2021). All of the biochar showed hydrophobic (lipophobicity) characteristics in PVA aqueous solution, which was mainly aqueous solution because there was less solute (PVA) in solution. Due to the addition of solute (PVA), the degree of hydrophobic (lipophobicity) was slightly reduced, which was consistent with the results of WCA.

### 3.2. Characterization of LTS and BPC

The synthesis of liquefied tobacco stem (LTS) as shown in Fig. 3a. The average molecular weight of LTS was 232 g/mol (Fig. S4a), indicating TS was successfully decomposed into small molecular compounds by liquefaction, which is conducive to the subsequent synthesis reaction of BPC (Chen et al., 2023). Moreover, the GC-MS analysis of LTS composition has unveiled that the macromolecular substance TS, composed of hemicellulose, cellulose, and lignin (Mw = 8064), was decomposed during pyrolysis (Sun et al., 2019). The decomposition products include small molecular compounds such as Hexaethylene glycol and hydroxyethoxy ethanol, with specific details found in Table S3. The hydroxyl value of TS reached 237.96 mg KOH/g (Table S4), which indicated that LTS was more likely to react with isocyanate to form BPC. A bio-based polyurethane coating (BPC) with hydrophobic properties was prepared and applied to the outermost coating of fertilizers, and the synthesis process of BPC as shown in Fig. 3b. BPC was prepared by the reaction of LTS with castor oil and PAPI. The BPC film was obtained by film forming experiment on polytetrafluoroethylene plate, and its WCA was determined to be 95° (Fig. S4b), which was a hydrophobic coating material.

To further confirm the successful synthesis of LTS and BPC, FTIR was used to analyze the surface functional groups of TS, LTS, mixed polyols, CO and BPC, as shown in Fig. 4a. For TS, the characteristic peaks of -OH, C-C and C-O bonds correspond to3437 $cm^{-1}$, 1381 $cm^{-1}$, 1043 $cm^{-1}$, respectively. For polyols (LTS, CO, mixed polyols), the absorption peak at 3420 $cm^{-1}$ indicated the stretching vibration of -OH, while the peak at 2919 $cm^{-1}$ and 2850 $cm^{-1}$ indicated the symmetric and asymmetric stretching vibration of C-H (Lee et al., 2017). The absorption peak at 1739 $cm^{-1}$ correspond to the stretching vibration of -COO-, indicating the decomposition of cellulose (Ma et al., 2018). The broadband peak at 1088 $cm^{-1}$ can be attributed to the stretching vibration of the C-O bond, indicating that the product of the liquefied biomass is a polyether polyol (Wang et al., 2023). For BPC, the weak characteristic peak at 3420 $cm^{-1}$ correspond to less -OH stretching and N-H stretching vibration, while the characteristic peak at 1739 $cm^{-1}$ and 1620 $cm^{-1}$ was C=O, and the absorption peak at 1527 $cm^{-1}$ was N-H bending vibration (Wang et al., 2022). The above analysis showed the successful synthesis TS and BPC. The degradation performance of BPC in soil was tested (Fig. 4b). It can be seen that BPC degraded 16 % in 120 days, which was higher than the degradation performance of polyurethane synthesized with castor oil alone (12 % degradation in 120 days) (Zuliani et al., 2022). The degradation rate of BPC fitted the zero-order kinetic equation, indicating the mass of BPC decreased steadily with time. The SEM before and after 120 days of BPC degradation was characterized (Fig. S5). Compared with BPC before degradation, more cracks and holes appeared in the surface regions of degraded BPC. This largely depends on the role of bacteria and fungi in the soil. Relevant studies have shown that

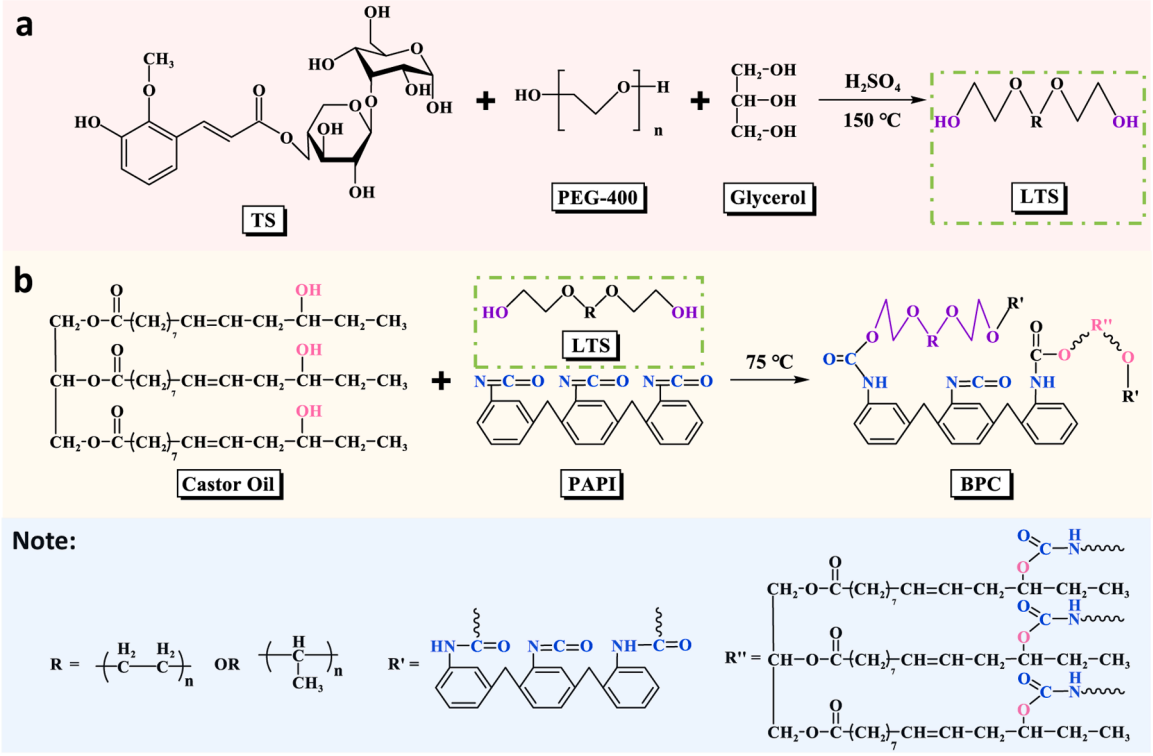


**Fig. 3.** Diagram of the synthesis process of (a) LTS and (b) BPC.

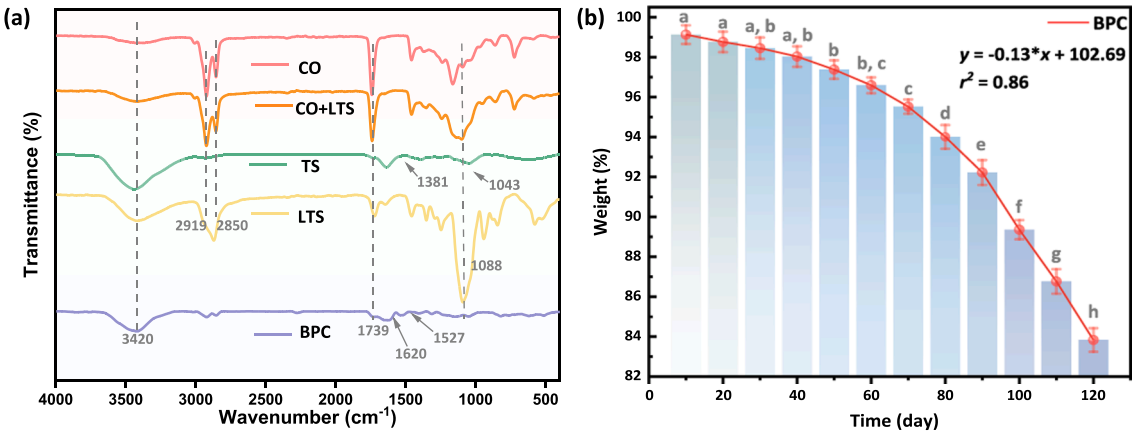


**Fig. 4.** (a) FTIR analysis of TS, polyols and BPC (b) degradability of the BPC in soil burial test.

microorganisms can selectively colonize and exhibit chemotaxis on the surface of coated materials, thus promoting the degradation of coated materials (Tian et al., 2024; Zhang et al., 2024). The high degradation performance of BPC provides a strategy for the application of green bio-based controlled-release fertilizer in agriculture.

### 3.3. Morphology analysis of BDCRFs

The SEM micrographs had shown that there were obvious pore structures on the surface of BDCRFs (Fig. 5). The pore structures may cause the coating layer to thin at the same rate of coating, allowing water to enter the kernel fertilizer easily, which leaded nutrients to released quickly (Zhang et al., 2017). It can be seen that TSF had fewer exposed holes compared with FWF and CSF, which was the result of the filling and covering of the surface coating materials. Through the cross-section of fertilizer, it's obviously that there were clear stratifications between the coating materials and the carbon materials. However, the FWB and CSB can be clearly seen in Fig. 5a2 and Fig. 5c2, respectively. There was a distinct gap between the CSB and the coating materials. For TS, the coating material was tightly bound to the carbon material in Fig. 5b2. This is due to the difference in the lipophilicity of different biochar, which resulting in the binding ability of biochar and the coating material was different (Zhang et al., 2023). The results had shown that the density of the coating was improved by the tight binding of TSB to BPC, and the TSF had fewer pore defects, enhancing the controlled-release performance of the coated fertilizer.

AFM were used to analyze the surface roughness and morphologies of the coating materials (Fig. S6). There were concentrated sunken poles on the surface of FWF, which indicated the existence of localized micro-holes. The surface of TSF were distributed with uniform and dense micro-bulges, indicating the higher surface roughness and uniform distribution of micro-holes. There were significant and discrete micro-bulges in CSF, showing the deep and uneven distributed micro-holes on the surface of CSF. It can be seen that TSF has the highest surface roughness and better hydrophobic properties compared with FWF and CSF, which is consistent with the results of WCA and SEM.

### 3.4. Nitrogen release and kinetics of BDCRFs

The initial and cumulative nitrogen-release curves of FWF, TSF and

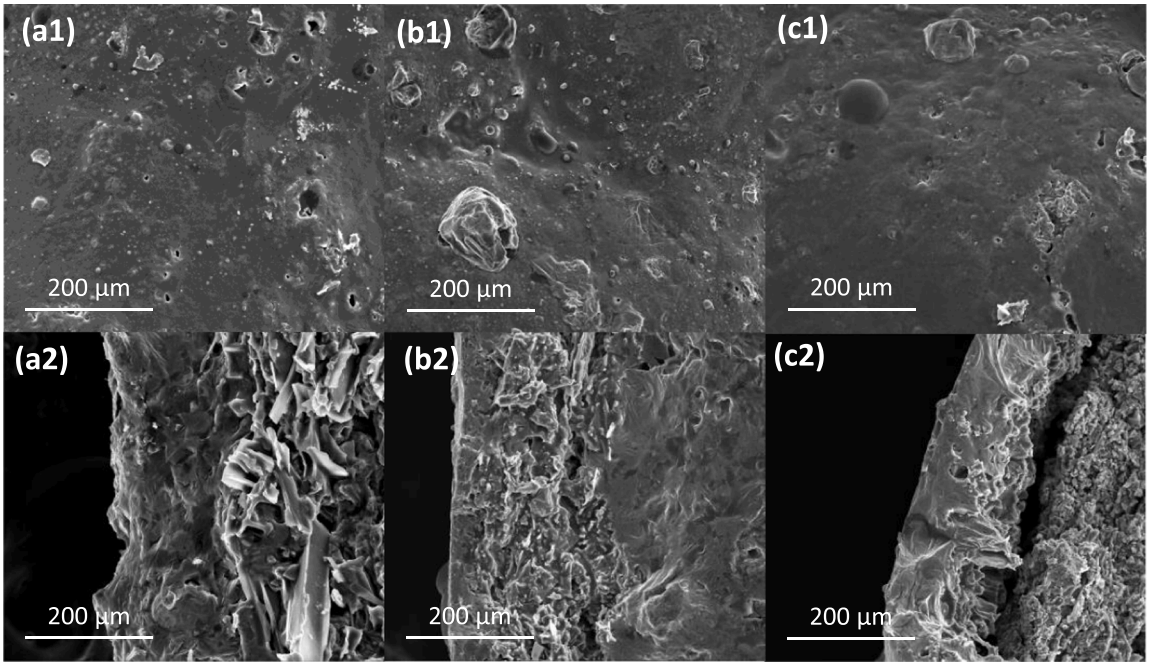


**Fig. 5.** SEM images of surface (a1) FWF, (b1) TSF and (c1) CSF and cross-section (a2) FWF, (b2) TSF and (c2) CSF.

CSF with 3 %, 5 % and 7 % polyurethane coating percentage were shown in Fig. 6. According to the initial release rate of fertilizers, it can be seen that the higher the coating rate, the lower the initial release rate of nutrients. The nutrient release rate of TSF was lower than FWF and CSF, indicating the TSF had better controlled-release performance than FWF and CSF. This can be attributed to the high hydrophobicity and lipophilicity of TSB, which enhance the nutrient release control performance of the coated fertilizer (Sankaranarayanan et al., 2021). According to the cumulative release rate of fertilizers, BDCRFs showed excellent controlled-release performance compared with NP. More than 80 % (96 % ± 4 %) of the nutrients in NP were released within 7 days, while the controlled-release longevity of CSF-3 % reached 70 days (82 % ± 4 %). FWF-3 % and TSF-3 % showed higher controlled-release performance compared with CSF-3 %, with 79 % ± 2 % and 71 % ± 2 % of nutrients released within 70 days, respectively. The coating percentage had great influence on the nutrient release rate of fertilizers. With the increasing of the coating percentage, the slower the nutrient release rate of fertilizer, the longer controlled-release performance (Wang et al., 2023). The coating rate increased from 3 % to 7 %, and the nutrient release longevity of CSF increased from 70 days to 124 days (The nitrogen release of TSF-7 % reaches 71 ± 2 % in 124 days). It can be seen that the nitrogen release rate of TSF was slower than FWF and CSF at the same percentage, which indicated the characteristics of biochar had the strong influence on fertilizer release characteristics (Zhang et al., 2023). The results had shown that TSF had the better nutrient controlled-release performance compared with FWF and CSF. This can be attributed to the lipophilicity of TSB formed a tight coating layer with the coating material, improving the controlled-release performance of TSF.

To investigate the release rule and mechanism of BDCRFs, the first-order kinetic equation, Higuchi equation and Ritger-Peppas equation were used to fit the release curve of nitrogen. The fitting parameters for nitrogen release kinetics of BDCRFs were listed (Table 2). All of the kinetics models described the process of nutrient release, and the correlation coefficient $R^2$ of Ritger-Peppas equation had shown that it was more able to represent the cumulative release rule and mechanism of nitrogen than the Higuchi equation and first-order kinetic equation (Das and Ghosh, 2022; Liu et al., 2020). Therefore, Ritger-Peppas equation was used to indicate the characteristics and mechanism of nutrient release in controlled-release fertilizers. The release performance of fertilizers was significantly affected by the amount of coating, the type of coating materials and the hydrophobic performance (Zhang et al., 2021; Zhao et al., 2020). For Ritger-Peppas equation, the value of $n \leq 0.43$, the nutrient release rule corresponded to the Fick diffusion, and the value of $0.43 \leq n \leq 0.85$, the diffusion is non-Fick diffusion, while the value of $0.85 \leq n$, the diffusion is Case-II transport. It can be seen in Table 2 that nutrient release of fertilizers with a coating amount of 3 % corresponded to the Fick diffusion, while nutrient release of fertilizers with a coating amount of 7 % corresponded to non-Fick diffusion. In addition, the controlled-release fertilizers with 5 % coating amount showed different release mechanisms due to different biochar with different hydrophobic and lipophilic, CSF-5 % was Fick diffusion, TSF-5 % and FWF-5 % were both non-Fick diffusion. The results had shown that high coating amount significantly enhanced the controlled-release performance of BDCRFs, which was consistent with the results of nutrient release. The high hydrophobic and lipophilic biochar can improve the controlled-release performance of CRFs. This may be due to the biochar cross-linking with BPC improved the hydrophobic properties of the coatings (An et al., 2021; Chen et al., 2018). Therefore, selecting the suitable biochar under the same controlled release time can greatly reduce the preparation cost of controlled-release fertilizer. Moreover, TSB had shown the lower diffusion kinetic constant $a$, $k$ and $K_H$ value in the equations at the

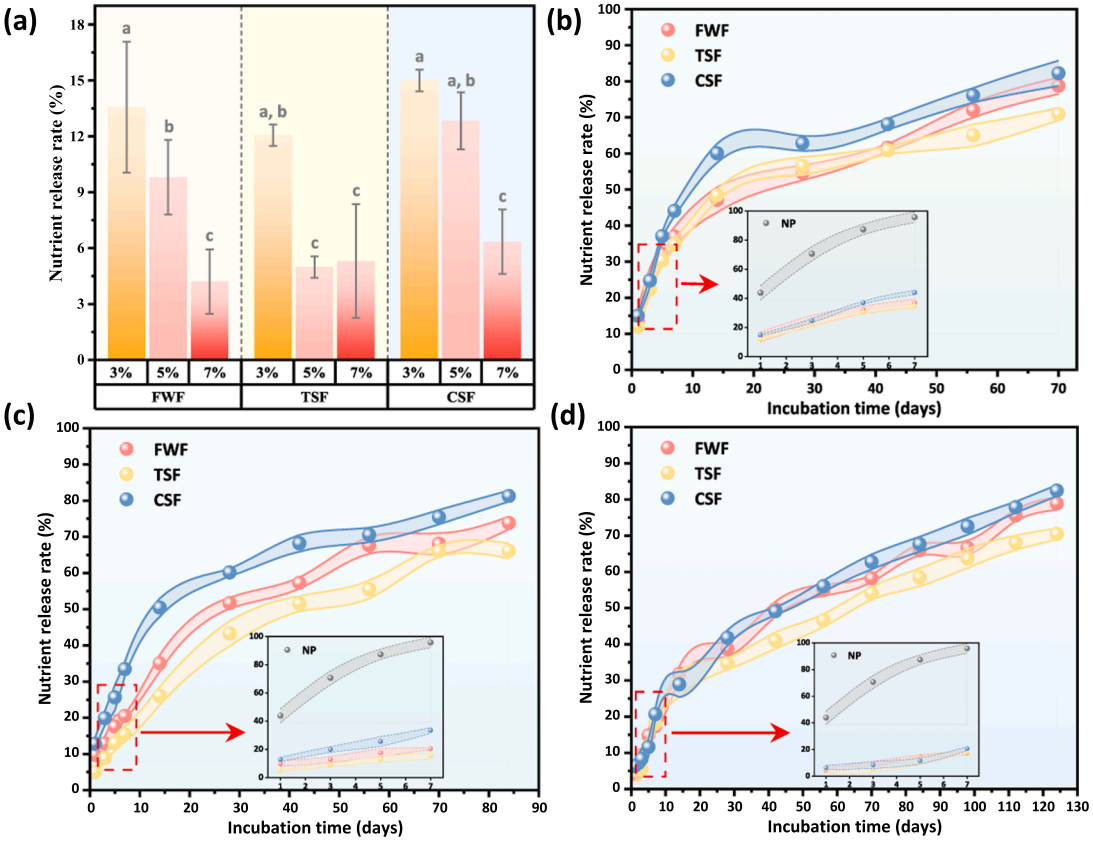


**Fig. 6.** (a) Initial release rate and cumulative release rate of N in column leaching of BDCRFs with (b) 3 %, (c) 5 %, (d) 7 % coating percentage. Note: the insertion chart shows the release of nitramine phosphorus (NP) and BDCRFs within 7 days.

**Table 2**
Fitting parameters of release kinetic equation of BDCRFs.

| Sample | Zero-order | | | First-order | | Higuchi | | Ritger-Peppas | | |
|---|---|---|---|---|---|---|---|---|---|---|
| | $a$ | $b$ | $R^2$ | $k$ | $R^2$ | $K_H$ | $R^2$ | $K$ | $n$ | $R^2$ |
| FWF−3 % | 0.82 | 26.32 | 0.90 | 0.11 | 0.88 | 1.64 | 0.89 | 17.42 | 0.35 | 0.99 |
| FWF−5 % | 0.79 | 17.06 | 0.91 | 0.05 | 0.98 | 1.57 | 0.90 | 9.54 | 0.47 | 0.99 |
| FWF−7 % | 0.56 | 15.64 | 0.93 | 0.03 | 0.97 | 1.13 | 0.92 | 7.43 | 0.49 | 0.98 |
| TSF−3 % | 0.76 | 26.10 | 0.83 | 0.12 | 0.96 | 1.49 | 0.81 | 17.50 | 0.33 | 0.97 |
| TSF−5 % | 0.74 | 11.37 | 0.93 | 0.03 | 0.99 | 1.47 | 0.92 | 6.11 | 0.55 | 0.98 |
| TSF−7 % | 0.51 | 13.46 | 0.94 | 0.02 | 0.96 | 1.03 | 0.93 | 6.23 | 0.51 | 0.99 |
| CSF−3 % | 0.82 | 31.66 | 0.81 | 0.13 | 0.94 | 1.64 | 0.78 | 21.62 | 0.32 | 0.95 |
| CSF−5 % | 0.76 | 26.23 | 0.85 | 0.08 | 0.96 | 1.52 | 0.83 | 16.23 | 0.37 | 0.97 |
| CSF−7 % | 0.60 | 15.40 | 0.93 | 0.02 | 0.98 | 1.20 | 0.93 | 7.09 | 0.51 | 0.99 |

same coating rate, which indicated the TSB significantly improved the controlled-release performance of fertilizers. The higher coating rate of controlled-release fertilizer with the same type of biochar also reduced the diffusion kinetic constants $a$, $k$ and $K_H$ value in the equations. This indicated the fertilizer with high coating rate had better controlled-release performance, which was consistent with the results of nutrient release.

### 3.5. Field experiment and economic evaluation

According to previous analysis, TSF showed excellent controlled-release performance, so TSF with different coating rates was applied to tobacco field experiment to explore the effect of BDCRFs on crop growth (Fig. 7). The biomass of tobacco was shown in Fig. 7a. Compared with CK (Fresh weight 214.6 ± 14.0 g, dry weight 28.0 ± 3.8 g), the biomass of tobacco in all fertilization groups was significantly increased. Specifically, it can be seen that the tobacco in the TSF-5 % group exhibited the largest biomass (fresh weight 700.5 ± 7.6 g, dry weight 98.2 ± 2.5 g) and slightly higher than that in the CF group (fresh weight 682.6 ± 32.1 g, dry weight 98.0 ± 1.5 g). This indicated that its nutrient release matched the nutrient requirements of tobacco and continued to supplement the nutrient requirements of tobacco growth. Leaf length, leaf width, Plant height and stem girth were important growth indexes of tobacco. The growth indexes under different fertilization treatments were shown in Fig. 7b-c. TSF group had better growth indexes than CF group and NP group. TSF-5 % group had the best growth indexes, with the leaf width reaching 30.9 ± 1.8 cm, leaf length reaching 60.9 ± 2.5 cm, plant height reaching 90.3 ± 3.9 cm and stem girth reaching 7.7 ± 0.4 cm. In the fast-effective fertilizers group, the tobacco growth indexes indicated a trend of CF > NP > CK in each group. Specifically, according to the order of CF, NP and CK groups, the tobacco growth indicators were as follows: the leaf width was 26.6 ± 1.2 > 23.4 ± 1.1 > 17.2 ± 0.9; the leaf length was 57.0 ± 2.9 > 45.9 ± 3.0 > 34.5 ± 0.8; the plant height was 86.7

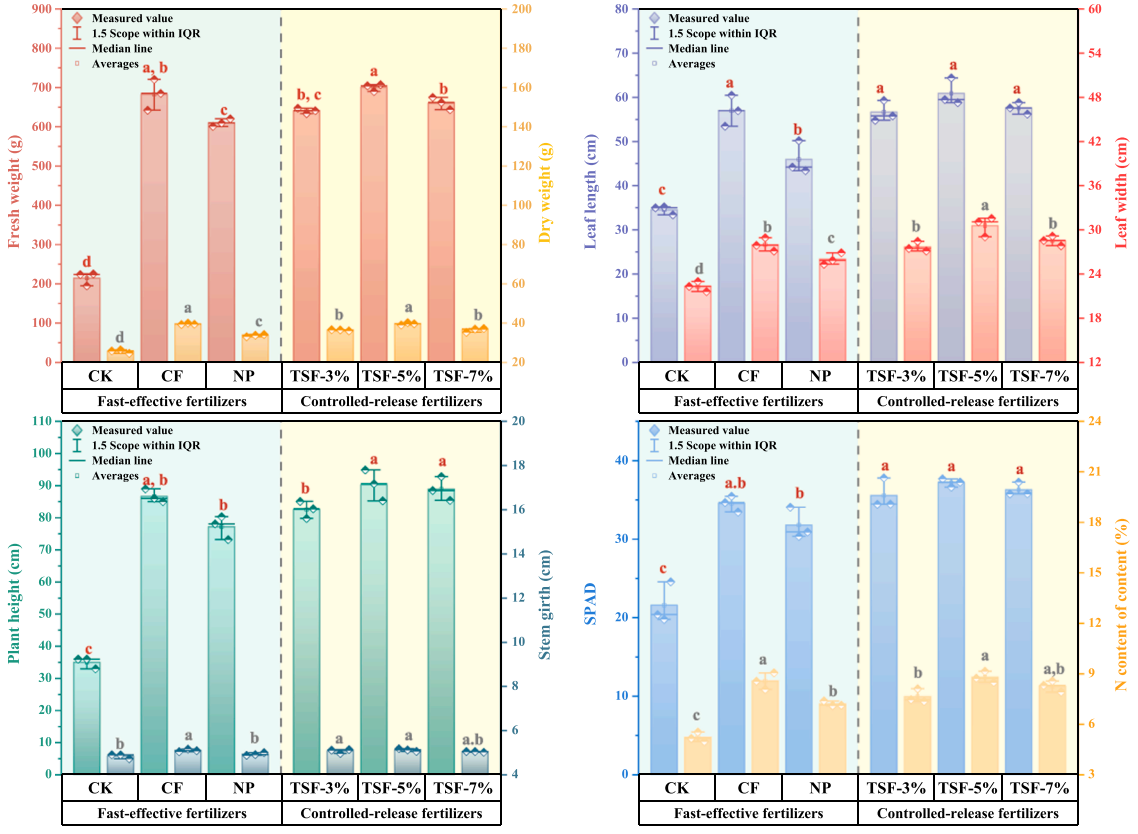


**Fig. 7.** The BDCRFs application in tobacco field experiment: (a) fresh and dry weight, (b) leaf length and width, (c) plant height and stem girth, (d) SPAD and nitrogen content of plants. Note: lowercase letters indicate significant differences among treatments ($p < 0.01$).

$\pm$ 1.7 > 77.2 $\pm$ 3.0 > 35.0 $\pm$ 1.4; The stem girth was 7.6 $\pm$ 0.3 > 6.4 $\pm$ 0.4 > 5.8 $\pm$ 0.6. The SPAD and nitrogen content of tobacco reflected the nutrient status of different treatments (Fig. 7d). CK showed the lowest SPAD (21.6 $\pm$ 2.1) and nitrogen content (5 $\pm$ 1 %), while TSF-5 % had the highest SPAD (37.2 $\pm$ 0.4) and nitrogen content (13 $\pm$ 1 %). There was little difference between the nitrogen content of CF (12 $\pm$ 1 %) and TSF-5 % (13 $\pm$ 1 %). The results showed that the nutrient release of TSF-5 % can meet the nutrient demand of tobacco growth, promote the absorption and utilization of nutrients, reduce nutrient leaching and improve fertilizer utilization rate. It is worth mentioning that the conventional fertilization of tobacco requires manual multiple top dressing at different times, while BDCRFs only needs to be applied once before tobacco transplanting, which greatly reduces labor costs and provides a theoretical reference for the development and utilization of novel fertilizers. Fig. S7 shows the photos of tobacco field experiment maturation in each group.

The results of the economic evaluation revealed that the production costs of the fertilizers developed in this work were significantly lower than those of commercial slow/controlled-release fertilizers (Table 3). The total production of TSF-3 %, TSF-5 % and TSF-7 % is 2.27 USD/kg, 2.37 USD/kg and 2.47 USD/kg respectively. The highly effective TSF-5 % reduced the preparation cost by 9.14 USD/kg and 3.00 USD/kg compared to 1-C-CRFs and 2-C-CRFs, respectively. In addition, commercial CRFs mainly use urea as the fertilizer core, which was also used in a large proportion of the studies (Azeem et al., 2014). This limits the use of CRFs with urea as the core (some crops are not suitable for urea application, such as tobacco). BDCRFs with nitramine phosphorus as fertilizer core can be applied to tobacco, which needs multiple topdressing crops (Jiang et al., 2025). BDCRFs are expected to be scaled up to develop a market for the application in crops such as tobacco due to their demand and low cost of production. The photographs of (a) TS, (b) LTS, (c) BPC, (d) FWF-5 %, (e) TSF-5 % and (f) CSF-5 % as show in Fig. S8.

## 4. Conclusion

An environmentally friendly controlled-release fertilizer (BDCRFs) with low-cost and excellent performance was developed through the double-coating of biochar and bio-based polyurethane. The physico-chemical properties and morphology of biochar and BPC were studied, while the controlled-release performance of BDCRFs were evaluated and compared. The results demonstrated that the coupling of biochar and bio-based polyurethane enables long-term, stable nutrient release in BDCRFs, following the Ritger-Peppas model. Moreover, the application of BDCRFs in tobacco planting has achieved excellent results. However, challenges remain in terms of scale production, given that the synthesis process involves the coupling of multiple materials and is more complex than standard coated CRFs. The strategy of using biochar and bio-based polyurethane in CRFs has proven to be a feasible method for enhancing controlled-release performance and achieving green, low-cost production. The application prospect of BDCRFs in the future can be further improved by optimizing the synthesis process. In the context of circular and sustainable agriculture, the BDCRFs prepared in this work are derived from tobacco field waste and effectively meet the nutrient requirements of tobacco. The application effect of BDCRFs in other crops and the performance of BDCRFs prepared from more agricultural wastes need to be further investigated. Future research should focus on optimizing the formulation of BDCRFs to broaden the agricultural applications, while also addressing the diverse needs of crops in sustainable agricultural systems.

## CRediT authorship contribution statement

**Nan Zhou:** Supervision. **Wei Luo:** Writing – review & editing, Supervision. **Yan Ying He:** Visualization, Data curation. **Ying Zhen Huang:** Data curation. **Jian Hua Li:** Data curation, Software, Writing – review & editing. **Zhi Chao Xiang:** Visualization, Data curation. **Xin Tang:** Writing – original draft, Methodology, Formal analysis, Conceptualization, Writing – review & editing. **Jia Yi Yang:** Software, Investigation, Data curation. **Zhi Zhou:** Writing – review & editing, Supervision, Resources.

**Table 3**
The economic evaluation of BDCRFs.

| Item | TSF-3 % (USD/kg) | TSF-5 % (USD/kg) | TSF-7 % (USD/kg) | 1-C-CRFs[a] (USD/kg) | 2-C-CRFs[b] (USD/kg) |
|---|---|---|---|---|---|
| Electricity | 0.50 | 0.50 | 0.50 | - | - |
| Castor oil | 0.02 | 0.03 | 0.04 | - | - |
| PEG−400 | 0.11 | 0.18 | 0.25 | - | - |
| Glycerol | 0.01 | 0.02 | 0.03 | - | - |
| Attapulgite | 0.45 | 0.45 | 0.45 | - | - |
| PVA (4 %) | 0.26 | 0.26 | 0.26 | - | - |
| $H_2SO_4$ | 0.01 | 0.01 | 0.01 | - | - |
| PAPI | 0.01 | 0.02 | 0.03 | - | - |
| TS | 0.08 | 0.08 | 0.08 | - | - |
| NP | 0.83 | 0.83 | 0.83 | - | - |
| Total | 2.27 | 2.37 | 2.47 | 11.51[c] | 5.37[d] |

*a*: 1-C-CRFs: the first type of commercial fertilizer.
*b*: 2-C-CRFs: the second type of commercial fertilizer.
*c*: the data derived from the study of Tanan et al. (Tanan et al., 2021).
*d*: the data was based on the average selling price of three classic controlled release fertilizers (OSMOCOTE 5.93 USD/kg, NUTRICOTE 7.44 USD/kg, JINZHENGDA controlled-release fertilizer 2.75 USD/kg).

## Declaration of Competing Interest

The authors declare that they have no known competing financial interests or personal relationships that could have appeared to influence the work reported in this paper.

## Acknowledgements

The authors gratefully acknowledge funds from the National Natural Science Foundation of China (Grant 51974123), the Key R&D Projects in Hunan Province (2021SK2047, and 2022NK2044), the Natural Science Foundation of Hunan Province, China (Grant 2023JJ40307), the Earmarked fund for China Agriculture Research System (CARS-01-27), the science and technology innovation Program of Hunan Province (2022WZ1022), 2022 National Center of Technology Innovation for Saline-Alkali Tolerant Rice Functional Improvement Project (No. 2022PT1005), Research on resource utilization and environmental pollution control of rural organic solid waste (xczx-2024131), Study and demonstration of tobacco field waste Resource utilization in Hengyang Area (HYYC2023KJ31), Study and application of nitrogen controlled release for tobacco based on porous adsorption and novel coating (CS2022KJ01), Hunan Engineering Research Center for Biochar, Hunan Optical Agriculture Engineering Technology Research Center (2018TP2003).

## Appendix A. Supporting information

Supplementary data associated with this article can be found in the online version at doi:10.1016/j.indcrop.2024.120296.

## Data availability

Data will be made available on request.

## References

An, T., Cheng, H., Qin, Y., Su, W., Deng, H., Wu, J., Liu, Z., Guo, X., 2021. The dual mechanisms of composite biochar and biofilm towards sustainable nutrient release

control of phosphate fertilizer: effect on phosphorus utilization and crop growth. J. Clean. Prod. 311, 127329. https://doi.org/10.1016/j.jclepro.2021.127329.
Azeem, B., KuShaari, K., Man, Z.B., Basit, A., Thanh, T.H., 2014. Review on materials & methods to produce controlled release coated urea fertilizer. J. Control. Release 181, 11–21. https://doi.org/10.1016/j.jconrel.2014.02.020.
Bera, T., Purakayastha, T.J., Patra, A.K., Datta, S.C., 2017. Comparative analysis of physicochemical, nutrient, and spectral properties of agricultural residue biochars as influenced by pyrolysis temperatures. J. Mater. Cycles Waste Manag. 20, 1115–1127. https://doi.org/10.1007/s10163-017-0675-4.
Brzoska, J., Smorawska, J., Głowińska, E., Datta, J., 2024. A green route for high-performance bio-based polyurethanes synthesized from modified bio-based isocyanates. Ind. Crops Prod. 222. https://doi.org/10.1016/j.indcrop.2024.119542.
Carneiro, J.Sd.S., Lustosa Filho, J.F., Nardis, B.O., Ribeiro-Soares, J., Zinn, Y.L., Melo, L. C.A., 2018. Carbon stability of engineered biochar-based phosphate fertilizers. ACS Sustain. Chem. Eng. 6, 14203–14212. https://doi.org/10.1021/acssuschemeng.8b02841.
Chen, S., Yang, M., Ba, C., Yu, S., Jiang, Y., Zou, H., Zhang, Y., 2018. Preparation and characterization of slow-release fertilizer encapsulated by biochar-based waterborne copolymers. Sci. Total Environ. 615, 431–437. https://doi.org/10.1016/j.scitotenv.2017.09.209.
Chen, X., Guo, T., Mo, X., Zhang, L., Wang, R., Xue, Y., Fan, X., Sun, S., 2023. Reduced nutrient release and greenhouse gas emissions of lignin-based coated urea by synergy of carbon black and polysiloxane. Int. J. Biol. Macromol. 231, 123334. https://doi.org/10.1016/j.ijbiomac.2023.123334.
da Cruz, D.F., Bortoletto-Santos, R., Guimarães, G.G.F., Polito, W.L., Ribeiro, C., 2017. Role of polymeric coating on the phosphate availability as a fertilizer: insight from phosphate release by castor polyurethane coatings. J. Agric. Food Chem. 65, 5890–5895. https://doi.org/10.1021/acs.jafc.7b01686.
Das, S.K., Ghosh, G.K., 2022. Hydrogel-biochar composite for agricultural applications and controlled release fertilizer: a step towards pollution free environment. Energy 242, 122977. https://doi.org/10.1016/j.energy.2021.122977.
Dong, H., Luo, W., Yan, X., Li, B., Hu, J., Huang, S., Xia, M., Zhong, M.-e, Tang, Q., Zhou, Z., Zhou, N., 2022. Production of catalytic-upgraded pyrolysis products from oiltea camellia shell and polypropylene using NiCe-X/$Al_2O_3$ and $ZrO_2$ catalyst (X = Fe, Co). Fuel 325, 124812. https://doi.org/10.1016/j.fuel.2022.124812.
Dong, H., Tang, S., Zhang, L., Tong, Z., Wu, Z., Zhan, P., Shao, L., Qing, Y., Liu, J., 2023. Wood-derived bio-coating materials incorporating hydrophobic lignin and hierarchically porous biochar for high-efficiency coating slow-release fertilizers. Int. J. Biol. Macromol. 242, 124769. https://doi.org/10.1016/j.ijbiomac.2023.124769.
Dugdug, A.A., Chang, S.X., Ok, Y.S., Rajapaksha, A.U., Anyia, A., 2018. Phosphorus sorption capacity of biochars varies with biochar type and salinity level. Environ. Sci. Pollut. Res. 25, 25799–25812. https://doi.org/10.1007/s11356-018-1368-9.
Fan, M., Li, C., Shao, Y., Zhang, S., Gholizadeh, M., Hu, X., 2022. Pyrolysis of cellulose: Correlation of hydrophilicity with evolution of functionality of biochar. Sci. Total Environ. 825. https://doi.org/10.1016/j.scitotenv.2022.153959.
González, M.E., Cea, M., Medina, J., González, A., Diez, M.C., Cartes, P., Monreal, C., Navia, R., 2015. Evaluation of biodegradable polymers as encapsulating agents for the development of a urea controlled-release fertilizer using biochar as support material. Sci. Total Environ. 505, 446–453. https://doi.org/10.1016/j.scitotenv.2014.10.014.
Hu, H., Li, P., Tong, Y.W., Li, J., He, Y., 2024. Reutilization recovered nutrients from wastewater by synthesizing eco-friendly slow-release hydrogel fertilizer for sustainable vegetable production. Chem. Eng. J. 499. https://doi.org/10.1016/j.cej.2024.155943.
Jia, Y., Hu, Z., Mu, J., Zhang, W., Xie, Z., Wang, G., 2020. Preparation of biochar as a coating material for biochar-coated urea. Sci. Total Environ. 731, 139063. https://doi.org/10.1016/j.scitotenv.2020.139063.
Jiang, Y., Gu, K., Song, L., Zhang, C., Liu, J., Chu, H., Yang, T., 2025. Fertilization and rotation enhance tobacco yield by regulating soil physicochemical and microbial properties. Soil Tillage Res. 247. https://doi.org/10.1016/j.still.2024.106364.
Kassem, I., Ablouh, E.-H., El Bouchtaoui, F.-Z., Jaouahar, M., El Achaby, M., 2024. Polymer coated slow/ controlled release granular fertilizers: fundamentals and research trends. Prog. Mater. Sci. 144. https://doi.org/10.1016/j.pmatsci.2024.101269.
Lee, M., Koo, J., Ki, H., Lee, K.H., Min, B.H., Lee, Y.C., Kim, J.H., 2017. Phase separation and electrical conductivity of nanocomposites made of ether-/ester-based polyurethane blends and carbon nanotubes. Macromol. Res. 25, 231–242. https://doi.org/10.1007/s13233-017-5032-x.
Liu, L., Ni, Y., Zhi, Y., Zhao, W., Pudukudy, M., Jia, Q., Shan, S., Zhang, K., Li, X., 2020. Sustainable and biodegradable copolymers from SO2 and renewable eugenol: a novel urea fertilizer coating material with superio slow release performance. Macromolecules 53, 936–945. https://doi.org/10.1021/acs.macromol.9b02202.
Ma, C., Zhang, F., Liu, H., Wang, H., Hu, J., 2022. Thermogravimetric pyrolysis kinetics study of tobacco stem via multicomponent kinetic modeling, Asym2sig deconvolution and combined kinetics. Bioresour. Technol. 360, 127539. https://doi.org/10.1016/j.biortech.2022.127539.
Ma, X., Chen, J., Yang, Y., Su, X., Zhang, S., Gao, B., Li, Y.C., 2018. Siloxane and polyether dual modification improves hydrophobicity and interpenetrating polymer network of bio-polymer for coated fertilizers with enhanced slow release characteristics. Chem. Eng. J. 350, 1125–1134. https://doi.org/10.1016/j.cej.2018.06.061.
Madhubashani, A.M.P., Giannakoudakis, D.A., Amarasinghe, B.M.W.P.K., Rajapaksha, A. U., Pradeep Kumara, P.B.T., Triantafyllidis, K.S., Vithanage, M., 2021. Propensity and appraisal of biochar performance in removal of oil spills: A comprehensive review. Environ. Pollut. 288, 117676. https://doi.org/10.1016/j.envpol.2021.117676.
Marcińczyk, M., Oleszczuk, P., 2022. Biochar and engineered biochar as slow- and controlled-release fertilizers. J. Clean. Prod. 339, 130685. https://doi.org/10.1016/j.jclepro.2022.130685.
Mohamed, R.R., Fahim, M.E., Soliman, S.M.A., 2022. Development of hydrogel based on Carboxymethyl cellulose/poly(4-vinylpyridine) for controlled releasing of fertilizers. BMC Chem. 16, 52. https://doi.org/10.1186/s13065-022-00846-6.
Muvhiiwa, R., Mawere, E., Moyo, L.B., Tshuma, L., 2021. Utilization of cellulose in tobacco (Nicotiana tobacum) stalks for nitrocellulose production. Heliyon 7. https://doi.org/10.1016/j.heliyon.2021.e07598.
Nielsen, M.B., Clausen, L.P.W., Cronin, R., Hansen, S.F., Oturai, N.G., Syberg, K., 2023. Unfolding the science behind policy initiatives targeting plastic pollution. Micro Nanoplast. 3. https://doi.org/10.1186/s43591-022-00046-y.
Papadopoulou, V., Kosmidis, K., Vlachou, M., Macheras, P., 2006. On the use of the Weibull function for the discernment of drug release mechanisms. Int. J. Pharm. 309, 44–50. https://doi.org/10.1016/j.ijpharm.2005.10.044.
Pariyar, P., Kumari, K., Jain, M.K., Jadhao, P.S., 2020. Evaluation of change in biochar properties derived from different feedstock and pyrolysis temperature for environmental and agricultural application. Sci. Total Environ. 713, 136433. https://doi.org/10.1016/j.scitotenv.2019.136433.
Prasad, M., Tzortzakis, N., McDaniel, N., 2018. Chemical characterization of biochar and assessment of the nutrient dynamics by means of preliminary plant growth tests. J. Environ. Manag. 216, 89–95. https://doi.org/10.1016/j.jenvman.2017.04.020.
Sankaranarayanan, S., Lakshmi, D.S., Vivekanandhan, S., Ngamcharussrivichai, C., 2021. Biocarbons as emerging and sustainable hydrophobic/oleophilic sorbent materials for oil/water separation. Sustain. Mater. Technol. 28, e00268. https://doi.org/10.1016/j.susmat.2021.e00268.
Shaaban, A., Se, S.-M., Mitan, N.M.M., Dimin, M.F., 2013. Characterization of biochar derived from rubber wood sawdust through slow pyrolysis on surface porosities and functional groups. Procedia Eng. 68, 365–371. https://doi.org/10.1016/j.proeng.2013.12.193.
Sun, D., Wang, B., Wang, H.-M., Li, M.-F., Shi, Q., Zheng, L., Wang, S.-F., Liu, S.-J., Sun, R.-C., 2019. Structural elucidation of tobacco stalk lignin isolated by different integrated processes. Ind. Crops Prod. 140. https://doi.org/10.1016/j.indcrop.2019.111631.
Sun, T., Sun, Y., Huang, Q., Xu, Y., Jia, H., 2023. Sustainable exploitation and safe utilization of biochar: multiphase characterization and potential hazard analysis. Bioresour. Technol. 383, 129241. https://doi.org/10.1016/j.biortech.2023.129241.
Sun, X., Fu, H., Bao, M., Liu, W., Luo, C., Li, Y., Li, Y., Lu, J., 2022. Development of a new hydrophobic magnetic biochar for removing oil spills on the water surface. Biochar 4, 177–193. https://doi.org/10.1007/s42773-022-00184-9.
Tanan, W., Panichpakdee, J., Suwanakood, P., Saengsuwan, S., 2021. Biodegradable hydrogels of cassava starch-g-polyacrylic acid/natural rubber/polyvinyl alcohol as environmentally friendly and highly efficient coating material for slow-release urea fertilizers. J. Ind. Eng. Chem. 101, 237–252. https://doi.org/10.1016/j.jiec.2021.06.008.
Tian, H., Wang, L., Zhu, X., Zhang, M., Li, L., Liu, Z., Abolfathi, S., 2024. Biodegradation of microplastics derived from controlled release fertilizer coating: selective microbial colonization and metabolism in plastisphere. Sci. Total Environ. 920. https://doi.org/10.1016/j.scitotenv.2024.170978.
Wang, C., Song, S., Yang, Z., Liu, Y., He, Z., Zhou, C., Du, L., Sun, D., Li, P., 2022. Hydrophobic modification of castor oil-based polyurethane coated fertilizer to improve the controlled release of nutrient with polysiloxane and halloysite. Prog. Org. Coat. 165, 106756. https://doi.org/10.1016/j.porgcoat.2022.106756.
Wang, C., Song, S., Du, L., Yang, Z., Liu, Y., He, Z., Zhou, C., Li, P., 2023. Nutrient controlled release performance of bio-based coated fertilizer enhanced by synergistic effects of liquefied starch and siloxane. Int. J. Biol. Macromol. 236, 123994. https://doi.org/10.1016/j.ijbiomac.2023.123994.
Wang, Y., Sun, M., Qiao, D., Li, J., Wang, Y., Liu, W., Bunt, C., Liu, H., Liu, J., Yang, X., 2021. Graft copolymer of sodium carboxymethyl cellulose and polyether polyol (CMC-g-TMN-450) improves the crosslinking degree of polyurethane for coated fertilizers with enhanced controlled release characteristics. Carbohydr. Polym. 272, 118483. https://doi.org/10.1016/j.carbpol.2021.118483.
Zhang, C., Wang, M., Chen, W.-H.H., Zhang, Y., Pétrissans, A., Pétrissans, M., Ho, S.-H. H., 2023. Superhydrophobic and superlipophilic biochar produced from microalga torrefaction and modification for upgrading fuel properties. Biochar 5, 18. https://doi.org/10.1007/s42773-023-00217-x.
Zhang, J., Balkovič, J., Azevedo, L.B., Skalský, R., Bouwman, A.F., Xu, G., Wang, J., Xu, M., Yu, C., 2018. Analyzing and modelling the effect of long-term fertilizer management on crop yield and soil organic carbon in China. Sci. Total Environ. 627, 361–372. https://doi.org/10.1016/j.scitotenv.2018.01.090.
Zhang, P., Bing, X., Jiao, L., Xiao, H., Li, B., Sun, H., 2022. Amelioration effects of coastal saline-alkali soil by ball-milled red phosphorus-loaded biochar. Chem. Eng. J. 431, 133904. https://doi.org/10.1016/j.cej.2021.133904.
Zhang, S., Yang, Y., Gao, B., Li, Y.C., Liu, Z., 2017. Superhydrophobic controlled-release fertilizers coated with bio-based polymers with organosilicon and nano-silica modifications. J. Mater. Chem. A 5, 19943–19953. https://doi.org/10.1039/c7ta06014a.
Zhang, S., Shen, T., Yang, Y., Ma, X., Gao, B., Li, Y.C., Wang, P., 2021. Novel environment-friendly superhydrophobic bio-based polymer derived from liquefied corncob for controlled-released fertilizer. Prog. Org. Coat. 151, 106018. https://doi.org/10.1016/j.porgcoat.2020.106018.
Zhang, Z., Zhang, Q., Yang, H., Cui, L., Qian, H., 2024. Mining strategies for isolating plastic-degrading microorganisms. Environ. Pollut. 346. https://doi.org/10.1016/j.envpol.2024.123572.

Zhao, X., Qi, X., Chen, Q., Ao, X., Guo, Y., 2020. Sulfur-modified coated slow-release fertilizer based on castor oil: synthesis and a controlled-release model. ACS Sustain. Chem. Eng. 8, 18044–18053. https://doi.org/10.1021/acssuschemeng.0c06056.
Zhu, Y., Cao, Y., Fu, B., Wang, C., Shu, S., Zhu, P., Wang, D., Xu, H., Zhong, N., Cai, D., 2024. Waste milk humification product can be used as a slow release nano-fertilizer. Nat. Commun. 15. https://doi.org/10.1038/s41467-023-44422-5.
Zuliani, A., Rapisarda, M., Chelazzi, D., Baglioni, P., Rizzarelli, P., 2022. Synthesis, characterization, and soil burial degradation of biobased polyurethanes. Polymers 14, 4948. https://doi.org/10.3390/polym14224948.